LETTER

ACUTE MYELOID LEUKEMIA

UTX loss alters therapeutic responses in KMT2A-rearranged acute myeloid leukemia

Xinyue Zhou[1,2], Pengcheng Zhang[1,2], Sajesan Aryal[1,2], Lixia Zhang[1,2] and Rui Lu[1,2]✉

Leukemia (2023) 37:226–230; https://doi.org/10.1038/s41375-022-01741-8

TO THE EDITOR:

Chromosomal rearrangements of the KMT2A or MLL gene (KMT2A-r) are found in ~10% acute myeloid leukemias (AML). KMT2A-r AML patients have a high rate of relapse and poor overall survival [1]. Recently, compounds targeting the MLL-fusion protein complex, such as DOT1L and Menin inhibitors, have shown promising preclinical efficacy [2]. However, molecular regulators of cellular response to these agents remain poorly understood. UTX (or KDM6A) is a histone H3K27 demethylase that plays a variety of roles in development and disease [3]. Recurrent loss-of-function UTX mutations have been found in many human cancers including leukemia [4]. Hematopoietic-specific loss of Utx in mouse induces spontaneous leukemia by regulating enhancer activity and chromatin remodeling [5]. UTX-null leukemia shows greater resistance to chemotherapy agents [6]. However, the impact of UTX on drug resistance of KMT2A-r AML has not been explored.

To investigate the potential role of UTX in regulating drug resistance in KMT2A-r AML, we utilized CRISPR/Cas9 approach to establish isogenic wildtype and knockout lines of UTX in the KMT2A-r OCI-AML2 cells (Fig. 1A). We next performed compound treatment studies with a collection of epigenetic modulator inhibitors that have demonstrated efficacy in preclinical models of KMT2A-r AML [7], which include DOT1L inhibitors SGC0946 and EPZ-5676, Menin-MLL inhibitor VTP50469, EZH2 inhibitor GSK126, bromodomain inhibitor JQ1, type I PRMT inhibitor MS023, and LSD1 inhibitor ORY-1001 (Fig. S1A). While UTX depletion did not affect the cellular responses to many of these epigenetic agents, loss of UTX specifically rendered resistance to inhibitors that target MLL complex, including DOT1L and Menin-MLL inhibitors (Fig. 1B and Fig. S1B). We later focused on DOT1L inhibitors because UTX depletion led to more profound resistance (Fig. 1B and Fig. S1B). We next used a genetic approach to investigate the vulnerability of UTX-proficient and -deficient cells to the loss of DOT1L protein. By using a competition-based growth assay, we found that UTX-null AML cells were significantly more resistant to DOT1L depletion (Fig. 1C). We further validated our observation by CRISPR/Cas9-mediated knockout of UTX in three KMT2A-r AML lines OCI-AML2, MOLM-13, and MV4-11 with two independent sgRNAs targeting UTX (Fig. S2). In each of the examined models, the loss of UTX conferred resistance to DOT1L inhibition (Fig. 1D–F). The IC_{50} concentration of DOT1L inhibitor SGC0946 increased by 2-to-10 folds in the cells with UTX depletion (Fig. 1G). We also validated this observation in a murine KMT2A-r AML model RN2 (MLL-AF9/$NRAS^{G12D}$) [8] cells, where Utx depletion consistently induced resistance to DOT1L inhibition (Fig. 1H–J). These data show that UTX is required for DOT1L sensitivity of KMT2A-r AML cells.

To further understand the drug resistance mechanism in leukemia cells with UTX loss, we performed transcriptome analysis in UTX wildtype and knockout OCI-AML2 cells treated with either DMSO or SGC0946. Principal component analysis shows that UTX knockout cells have a distinct transcriptional profile and were less responsive to DOT1L inhibitor treatment compared to UTX wildtype cells (Fig. 1K). Surprisingly, gene set variation analysis (GSVA) revealed that targets of MLL-fusion protein complex [9] were down-regulated by DOT1L inhibition in an equally effective way in both UTX wildtype and knockout cells (Fig. 1L). Indeed, we found that the canonical MLL-target genes, such as *HOXA* cluster genes, *MEIS1*, *MEF2C*, and *PBX3* were consistently inhibited by SGC0946 in UTX knockout cells (Fig. 1M), suggesting that UTX loss-mediated resistance to DOT1L inhibition is independent of MLL-target genes. Consistent with previous studies [10], DOT1L inhibition resulted a robust increase of hematopoietic lineage development and myeloid cell differentiation genes (Fig. 1L). Interestingly, these genes were down-regulated after UTX depletion and failed to be activated by DOT1L inhibitor in UTX-deficient cells (Figs. 1L, M). An overview of differentially expressed genes regulated by DOT1L inhibitor also support a global reduction of DOT1L inhibition-mediated gene activation in UTX-null KMT2A-r AML cells (Fig. S3). These data suggest that UTX is required for DOT1L inhibitor-mediated up-regulation of myeloid differentiation gene programs.

UTX is a conserved protein that consists an N-terminus tetratricopeptide repeat (TPR) domain which facilitates association with the MLL3/4 complex [11], a C-terminus catalytic Jumonji C (JmjC) domain, and a recently described core intrinsically disordered region between TPR and JmjC domains [12]. To investigate which domain(s) of UTX may play an important role in controlling the response to DOT1L inhibition, we employed an

[1]Department of Medicine, Division of Hematology/Oncology, University of Alabama at Birmingham Heersink School of Medicine, Birmingham, AL 35294, USA. [2]O'Neal Comprehensive Cancer Center, University of Alabama at Birmingham Heersink School of Medicine, Birmingham, AL 35294, USA. ✉email: ruilu1@uabmc.edu

Received: 19 July 2022 Revised: 14 October 2022 Accepted: 18 October 2022
Published online: 29 October 2022

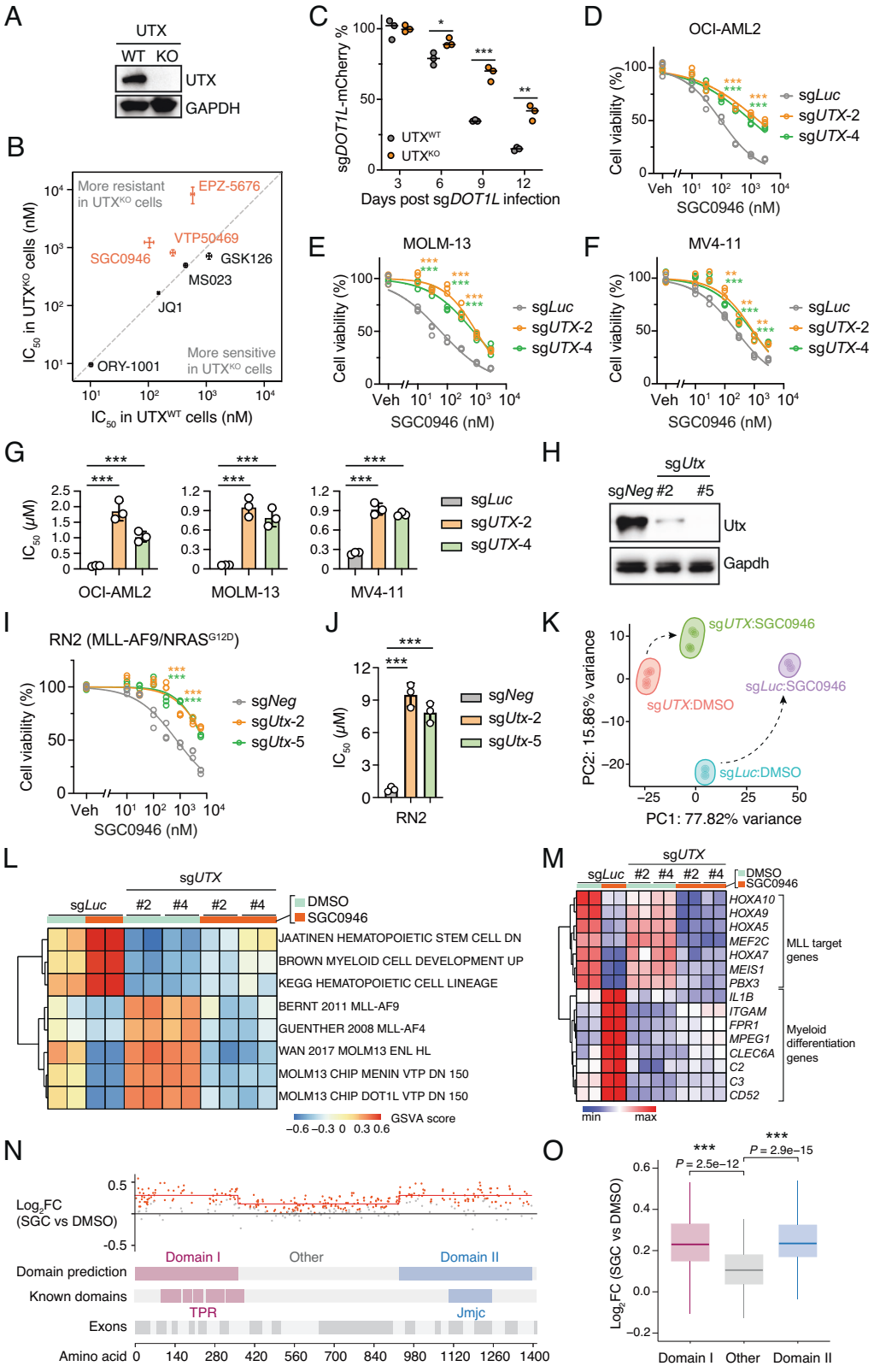
A
UTX
WT KO
UTX
GAPDH
B
More resistant in UTX^KO cells
More sensitive in UTX^KO cells
EPZ-5676
VTP50469
SGC0946
GSK126
MS023
JQ1
ORY-1001
IC50 in UTX^KO cells (nM)
IC50 in UTX^WT cells (nM)
C
sgDOT1L-mCherry %
UTX^WT
UTX^KO
Days post sgDOT1L infection
D
OCI-AML2
Cell viability (%)
SGC0946 (nM)
sgLuc
sgUTX-2
sgUTX-4
E
MOLM-13
F
MV4-11
G
IC50 (μM)
OCI-AML2
MOLM-13
MV4-11
H
sgUtx
sgNeg #2
#5
Utx
Gapdh
I
RN2 (MLL-AF9/NRAS^G12D)
sgNeg
sgUtx-2
sgUtx-5
J
RN2
K
sgUTX:SGC0946
sgLuc:SGC0946
sgUTX:DMSO
sgLuc:DMSO
PC2: 15.86% variance
PC1: 77.82% variance
L
sgUTX
sgLuc
#2
#4
DMSO
SGC0946
JAATINEN HEMATOPOIETIC STEM CELL DN
BROWN MYELOID CELL DEVELOPMENT UP
KEGG HEMATOPOIETIC CELL LINEAGE
BERNT 2011 MLL-AF9
GUENTHER 2008 MLL-AF4
WAN 2017 MOLM13 ENL HL
MOLM13 CHIP MENIN VTP DN 150
MOLM13 CHIP DOT1L VTP DN 150
GSVA score
M
HOXA10
HOXA9
HOXA5
MEF2C
HOXA7
MEIS1
PBX3
IL1B
ITGAM
FPR1
MPEG1
CLEC6A
C2
C3
CD52
MLL target genes
Myeloid differentiation genes
min
max
N
Log2FC (SGC vs DMSO)
Domain I
Other
Domain II
Domain prediction
Known domains
TPR
Jmjc
Exons
Amino acid
O
P = 2.5e−12
P = 2.9e−15
Log2FC (SGC vs DMSO)

Fig. 1 UTX loss confers resistance to DOT1L inhibition in KMT2A-r AML. A Western blot validation of UTX knockout in OCI-AML2 cells. **B** Plots of the half inhibition of cell growth (IC_{50}) of indicated compounds in suppressing in vitro growth of UTX wildtype and knockout OCI-AML2 cells. Compounds include DOT1L inhibitor SGC0946, DOT1L inhibitor EPZ-5676, Menin-MLL inhibitor VTP50469, EZH2 inhibitor GSK126, bromodomain inhibitor JQ1, type I PRMT inhibitor MS023, and LSD1 inhibitor ORY-1001. **C** Competitive growth assay of DOT1L knockout in UTX wildtype and knockout OCI-AML2 cells. sg*DOT1L* expression is linked to an mCherry gene. Graph shows the relative percentage of sg*DOT1L*-expressing cells at the indicated timepoints post sgRNA infection. The mCherry percentage was normalized to the day 3 measurement. Dose–response curves showing viabilities of OCI-AML2 (**D**), MOLM-13 (**E**), and MV4-11 (**F**) cells expressing indicated sgRNAs after treatment with DMSO vehicle (Veh) or various doses of SGC0946. Depicted are 9 days treatment for OCI-AML2, 6 days for MOLM-13, and 9 days for MV4-11. All cell viabilities were normalized to DMSO treatment. Showing are non-linear regression curves from data of three replicates. Statistical significance was assessed at selected doses using unpaired two-tailed Student's *t*-test. **G** Calculated IC_{50} values from **D**–**F**. Showing are mean IC_{50} values from data of three replicates ± SD. **H** Western blot validation of Utx knockout in RN2 cells. The sgRNA expression vector was used as a negative control (sg*Neg*). **I** Dose–response curves showing viabilities of RN2 cells expressing indicated sgRNAs after treatment with DMSO vehicle (Veh) or various doses of SGC0946 for 7 days. All cell viabilities were normalized to DMSO treatment. Showing are non-linear regression curves from data of three replicates. Statistical significance was assessed at selected doses using unpaired two-tailed Student's *t*-test. **J** Calculated IC_{50} values from **I**. Showing are mean IC_{50} values from data of three replicates ± SD. **K** Principal component analysis (PCA) of RNA-seq gene expression data from indicated OCI-AML2 cells treated with DMSO or 1 μM SGC0946 for 6 days. Two sgRNAs (sg*UTX*-2 and sg*UTX*-4) for UTX are shown. Dash lines denote the routes of SGC0946-induced transcriptome changes. **L** GSVA analysis showing transcriptome changes of gene sets associated with hematopoietic differentiation from Molecular Signatures Database (MsigDB) or published gene sets that are regulated by MLL complex components, such as MLL-fusion proteins, ENL, Menin, and DOT1L [9]. **M** Heatmap showing relative gene expression levels of representative MLL-target genes and myeloid differentiation genes, as measured by RNA-seq. **N** CRISPR tiling scan of UTX domains in OCI-AML2 cells treated with DMSO or SGC0946 for 15 days. Each dot depicts the amino acid position (x-axis) and the log2 fold change of sgRNA abundance in SGC0946-treated cells versus DMSO-treated cells (y-axis). Red dots indicate significantly differentially represented sgRNAs. The red line shows the segmented protein regions for predicted functional domains involved in regulating sensitivity to DOT1L inhibition. **O** Box plot showing log_2 fold changes of UTX sgRNAs located in predicted functional domains regions (Domain I and Domain II) as identified in **K**, comparing to other regions (Other). $^{*}P < 0.05$, $^{**}P < 0.01$, $^{***}P < 0.001$.

unbiased high-density CRISPR tiling scan approach [13], which allows a saturation mutagenesis screen of UTX coding exons in the context of DOT1L inhibition. We designed an sgRNA library which contains 365 all possible sgRNAs targeting UTX coding exons and 70 negative controls. We next transduced this library into Cas9-expressing OCI-AML2 cells for DMSO or SGC0946 treatment (Fig. S4A). As expected, a robust enrichment of UTX sgRNAs, but not the control sgRNAs, was observed post 10- or 15-day treatment of SGC0946 (Fig. S4B). By mapping these sgRNA sequences into the amino acid positions in UTX, we identified two domains, namely Domain I and Domain II, that may play a critical role in regulating DOT1L inhibitor sensitivity (Fig. 1N, O). Specifically, Domain I covers the N-terminus TPR domain, indicating an involvement of MLL3/4 complex, and Domain II hits the C-terminus JmjC domain, indicating a possible role of UTX's enzymatic activity in the regulation of leukemic cell response to DOT1L inhibition.

To define the target genes that are regulated by UTX in KMT2A-r AML, we performed chromatin immunoprecipitation assay of UTX, followed by deep sequencing (ChIP-seq). We found a significant overlap between genes bound by UTX and genes regulated by UTX as identified by RNA-seq ($n = 2128$, Chi-square $p < 2.2e{-}16$) (Fig. 2A). Consistent with previous studies showing that UTX can function as a transcriptional activator or repressor in leukemia cells [5], 1,408 UTX target genes were down-regulated and 720 UTX target genes were up-regulated upon UTX loss (Fig. S5). Interestingly, B-cell lymphoma 2-related protein A1 (*BCL2A1*) was among UTX-activated target genes (Fig. 2A and Fig. S5). ChIP-seq analysis showed that UTX binds to a distal region upstream of *BCL2A1* promoter (Fig. 2B). We also observed that H3K27ac, a histone mark that demarcates active enhancers and promoters, showed reduced signal at *BCL2A1* locus (Fig. 2B), which is in agreement of a previous report that UTX regulates histone acetylation of regions adjacent to its binding [5]. We further validated that UTX activates *BCL2A1* expression by performing UTX knockout in three independent human KMT2A-r AML models. In all cases, *BCL2A1* levels were significantly decreased after UTX knockout (Fig. 2C).

Since BCL2A1 has been demonstrated to be a key regulator of AML cell response to the BCL2 inhibitor venetoclax and cells expressing lower levels of *BCL2A1* are more sensitive to venetoclax [14]. We hypothesized that leukemias with UTX loss are more vulnerable to venetoclax treatment. Indeed, all examined AML cells showed hypersensitivity to venetoclax treatment upon loss of UTX, with 4-to-50-fold reduction of IC_{50} values (Fig. 2D, E). Consistently, depletion of Utx in the murine KMT2A-r RN2 cells led to significant reduction of expression of homologous mouse *Bcl2a1* genes (Fig. 2F), as well as increased cell sensitivity to venetoclax treatment (Fig. 2G, H). In human AML, we also observed a positive correlation between *UTX* and *BCL2A1* expression and a tendency of enhanced sensitivity to venetoclax in AML with low and medium *UTX* expression (Fig. S6). To examine the therapeutic effect of venetoclax in UTX-null AML in vivo, UTX wildtype and knockout OCI-AML2 cells were transplanted into immune-deficient recipient mice and treated with either vehicle control or venetoclax from day 5 to day 28 post engraftment. Importantly, while UTX loss did not significantly affect leukemia progression, UTX-deficient leukemia showed a remarkable reduction of engraftment upon venetoclax treatment (Fig. 2I, J). Venetoclax also significantly prolonged the survival of recipient mice bearing UTX-deficient leukemia (Fig. 2K).

Lastly, we sought to examine whether venetoclax treatment could overcome the resistance to DOT1L inhibition in UTX-deficient KMT2A-r AML cells. We leveraged a competition-based growth assay, where ~10% of AML cells were transduced with either control or UTX sgRNAs linked with an mCherry reporter, followed by treatment with DMSO, SGC0946, venetoclax, or a combination of both compounds (Fig. 2L). As expected, leukemia cells expressing UTX sgRNAs, but not the control sgRNA, displayed a growth advantage upon SGC0946 treatment and a growth disadvantage under treatment of venetoclax (Fig. 2M). Interestingly, a combination of venetoclax and SGC0946 completely abolished the resistance to SGC0946 in the UTX knockout cells (Fig. 2M), suggesting that BCL2 inhibitor may be used to overcome the resistance of UTX-deficient KMT2A-r AML cells to DOT1L inhibition.

Together, our data show a unique role of UTX in the regulation of therapeutic responses in KMT2A-r AML. Loss of UTX confers resistance to DOT1L and Menin inhibition but increases vulnerability to BCL2 inhibitor venetoclax, which could be used to overcome the therapeutic resistance to DOT1L inhibition. Because UTX is heterogeneously regulated in AML and loss of UTX is associated with disease relapse [6, 15], our results not only reveal dysregulation of UTX as a potential mechanism of resistance for

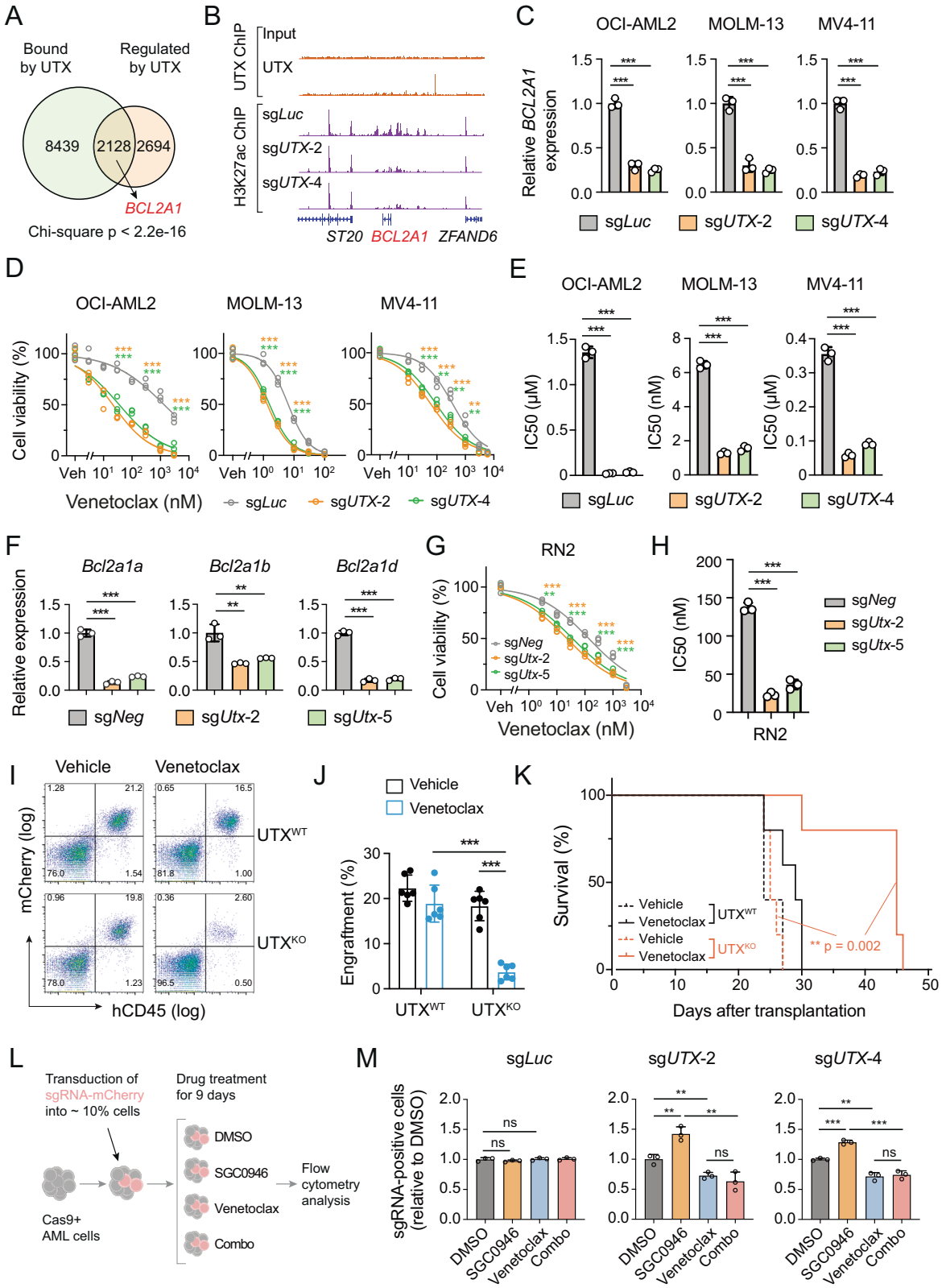
A
Bound by UTX
Regulated by UTX
8439
2128
2694
BCL2A1
Chi-square p < 2.2e-16
B
UTX ChIP
Input
UTX
H3K27ac ChIP
sgLuc
sgUTX-2
sgUTX-4
ST20
BCL2A1
ZFAND6
C
OCI-AML2
MOLM-13
MV4-11
Relative BCL2A1 expression
sgLuc
sgUTX-2
sgUTX-4
D
OCI-AML2
MOLM-13
MV4-11
Cell viability (%)
Venetoclax (nM)
sgLuc
sgUTX-2
sgUTX-4
E
OCI-AML2
MOLM-13
MV4-11
IC50 (μM)
IC50 (nM)
sgLuc
sgUTX-2
sgUTX-4
F
Bcl2a1a
Bcl2a1b
Bcl2a1d
Relative expression
sgNeg
sgUtx-2
sgUtx-5
G
RN2
Cell viability (%)
sgNeg
sgUtx-2
sgUtx-5
Venetoclax (nM)
H
IC50 (nM)
RN2
sgNeg
sgUtx-2
sgUtx-5
I
Vehicle
Venetoclax
mCherry (log)
UTXWT
UTXKO
hCD45 (log)
J
Vehicle
Venetoclax
Engraftment (%)
UTXWT
UTXKO
K
Survival (%)
Vehicle
Venetoclax
UTXWT
Vehicle
Venetoclax
UTXKO
** p = 0.002
Days after transplantation
L
Transduction of sgRNA-mCherry into ~ 10% cells
Drug treatment for 9 days
Cas9+ AML cells
DMSO
SGC0946
Venetoclax
Combo
Flow cytometry analysis
M
sgLuc
sgUTX-2
sgUTX-4
sgRNA-positive cells (relative to DMSO)
DMSO
SGC0946
Venetoclax
Combo

Fig. 2 UTX loss downregulates BCL2A1 and sensitizes KMT2A-r AML to BCL2 inhibitor. A Venn diagram showing the overlap of genes regulated by UTX and bound by UTX as identified from RNA-seq and ChIP-seq data, respectively. **B** UTX and H3K27ac ChIP-seq profiles at *BCL2A1* locus in OCI-AML2 cells (UTX ChIP-seq) or in OCI-AML2 cells expressing indicated sgRNAs (H3K27ac ChIP-seq). **C** RT-qPCR analysis of BCL2A1 mRNA levels in OCI-AML2, MOLM-13, and MV4-11 cells with stable expression of indicated sgRNAs. **D** Dose–response curves showing viabilities of OCI-AML2, MOLM-13, and MV4-11 cells expressing indicated sgRNAs after treatment with DMSO vehicle (Veh) or various doses of venetoclax. Depicted are 3 days treatment for OCI-AML2, 2 days for MOLM-13, and 4 days for MV4-11. All cell viabilities were normalized to DMSO treatment. Showing are non-linear regression curves from data of three replicates. Statistical significance was assessed at selected doses using unpaired two-tailed Student's *t*-test. **E** Calculated IC_{50} values from D. Showing are mean IC_{50} values from data of three replicates ± SD. **F** RT-qPCR analysis of mRNA expression of the mouse *BCL2A1* genes *Bcl2a1a*, *Bcl2a1b*, and *Blc2a1d* mRNA levels in Cas9-expressing RN2 cells with stable expression of indicated sgRNAs. **G** Dose–response curves showing viabilities of RN2 cells expressing indicated sgRNAs after treatment with DMSO vehicle (Veh) or various doses of venetoclax for 4 days. All cell viabilities were normalized to DMSO treatment. Showing are non-linear regression curves from data of three replicates. Statistical significance was assessed at selected doses using unpaired two-tailed Student's *t*-test. **H** Calculated IC_{50} values in RN2. Showing are mean IC_{50} values from data of three replicates ± SD. **I** Flow cytometry analysis of human CD45 and mCherry-positive cells in the peripheral blood of mice receiving UTX wildtype or knockout OCI-AML2 cells and treated with either vehicle or venetoclax for a duration of 4 weeks. **J** Percentage of human CD45 and mCherry double positive cells in the peripheral blood of mice described in **I**. **K** Kaplan–Meier survival curves of recipient mice described in **I**. **L** Schematic of competitive growth assay. OCI-AML2 cells were infected with mCherry-linked sgRNAs and treated with either DMSO, SGC0946 (1 μM), venetoclax (100 nM), or a combination of both compounds for 9 days, followed by flow cytometry measurement of mCherry-positive cells. **M** Bar plots showing relative enrichment of sgRNA-positive cells in OCI-AML2 cells described in **L**. Percentages of sgRNA-positive cells in each treatment were normalized to DMSO treatment control. $^{*}P < 0.05$, $^{**}P < 0.01$, $^{***}P < 0.001$, ns not significant.

DOT1L and Menin therapies, but also provide BCL2 inhibition as an alternative strategy to combat such acquired resistance.

DATA AVAILABILITY

The RNA-seq and ChIP-seq datasets have been deposited in the Gene Expression Omnibus (GEO) under the series number GSE214275.

REFERENCES

1. Meyer C, Kowarz E, Hofmann J, Renneville A, Zuna J, Trka J, et al. New insights to the MLL recombinome of acute leukemias. Leukemia. 2009;23:1490–9.
2. Chan AKN, Chen CW. Rewiring the epigenetic networks in MLL-rearranged leukemias: epigenetic dysregulation and pharmacological interventions. Front Cell Dev Biol. 2019;7:81.
3. Klose RJ, Kallin EM, Zhang Y. JmjC-domain-containing proteins and histone demethylation. Nat Rev Genet. 2006;7:715–27.
4. Wang L, Shilatifard A. UTX mutations in human cancer. Cancer Cell. 2019;35:168–76.
5. Gozdecka M, Meduri E, Mazan M, Tzelepis K, Dudek M, Knights AJ, et al. UTX-mediated enhancer and chromatin remodeling suppresses myeloid leukemogenesis through noncatalytic inverse regulation of ETS and GATA programs. Nat Genet. 2018;50:883–94.
6. Stief SM, Hanneforth AL, Weser S, Mattes R, Carlet M, Liu WH, et al. Loss of KDM6A confers drug resistance in acute myeloid leukemia. Leukemia. 2020;34:50–62.
7. Lu R, Wang GG. Pharmacologic targeting of chromatin modulators as therapeutics of acute myeloid leukemia. Front Oncol. 2017;7:241.
8. Zuber J, McJunkin K, Fellmann C, Dow LE, Taylor MJ, Hannon GJ, et al. Toolkit for evaluating genes required for proliferation and survival using tetracycline-regulated RNAi. Nat Biotechnol. 2011;29:79–83.
9. Krivtsov AV, Evans K, Gadrey JY, Eschle BK, Hatton C, Uckelmann HJ, et al. A Menin-MLL inhibitor induces specific chromatin changes and eradicates disease in models of MLL-rearranged leukemia. Cancer Cell. 2019;36:660–673.e611.
10. Daigle SR, Olhava EJ, Therkelsen CA, Majer CR, Sneeringer CJ, Song J, et al. Selective killing of mixed lineage leukemia cells by a potent small-molecule DOT1L inhibitor. Cancer Cell. 2011;20:53–65.
11. Shpargel KB, Starmer J, Wang C, Ge K, Magnuson T. UTX-guided neural crest function underlies craniofacial features of Kabuki syndrome. Proc Natl Acad Sci USA. 2017;114:E9046–e9055.
12. Shi B, Li W, Song Y, Wang Z, Ju R, Ulman A, et al. UTX condensation underlies its tumour-suppressive activity. Nature. 2021;597:726–31.
13. He W, Zhang L, Villarreal OD, Fu R, Bedford E, Dou J, et al. De novo identification of essential protein domains from CRISPR-Cas9 tiling-sgRNA knockout screens. Nat Commun. 2019;10:4541.
14. Zhang H, Nakauchi Y, Köhnke T, Stafford M, Bottomly D, Thomas R, et al. Integrated analysis of patient samples identifies biomarkers for venetoclax efficacy and combination strategies in acute myeloid leukemia. Nat Cancer. 2020;1:826–39.
15. Greif PA, Hartmann L, Vosberg S, Stief SM, Mattes R, Hellmann I, et al. Evolution of cytogenetically normal acute myeloid leukemia during therapy and relapse: an exome sequencing study of 50 patients. Clin Cancer Res. 2018;24:1716–26.

ACKNOWLEDGEMENTS

This work was supported in part by National Institutes of Health grants R01 CA259480, Concern Foundation, and Mark Foundation for Cancer Research. RL is an American Society of Hematology Scholar in Basic Science and a Research Scholar of American Cancer Society (RSG-22-036-01-DMC).

AUTHOR CONTRIBUTIONS

RL and XZ conceptualized the study and designed the experiments. XZ, PZ, SA, and LZ performed the experiments and interpreted the data. XZ and RL wrote the manuscript with inputs from all authors.

COMPETING INTERESTS

The authors declare no competing interests.

ADDITIONAL INFORMATION

Supplementary information The online version contains supplementary material available at https://doi.org/10.1038/s41375-022-01741-8.

Correspondence and requests for materials should be addressed to Rui Lu.

Reprints and permission information is available at http://www.nature.com/reprints

Publisher's note Springer Nature remains neutral with regard to jurisdictional claims in published maps and institutional affiliations.